Intermetallics 22 (2012) 17–23

Contents lists available at SciVerse ScienceDirect

Intermetallics

journal homepage: www.elsevier.com/locate/intermet

Thermodynamic properties of Laves phases in the Mg–Al–Ca system at finite temperature from first-principles

Hui Zhang*, Shun-Li Shang, Yi Wang, Long-Qing Chen, Zi-Kui Liu

Department of Materials Science and Engineering, The Pennsylvania State University, 304 Steidle Building, University Park, PA 16802, USA

ARTICLE INFO

Article history:
Received 29 December 2010
Received in revised form
10 August 2011
Accepted 26 August 2011
Available online 24 November 2011

Keywords:
A. Laves phases
B. Thermodynamic and thermochemical properties
E. Ab-initio calculations

ABSTRACT

First-principles calculations are employed to investigate the structural and thermodynamic properties of binary Laves phases (C14, C15 and C36 structures) in the Mg–Al–Ca system. The enthalpies of formation at 0 K are predicted. The vibrational contributions to Helmholtz free energy for the stable C14-Mg_2Ca and C15-Al_2Ca phases are determined using both first-principles phonon calculations and Debye–Grüneisen model. The predicted thermodynamic properties of the stable phases, including enthalpy, entropy, bulk modulus, heat capacity, and thermal expansion coefficient, agree well with available experimental data. For the other nonstable phases, the thermodynamic properties are estimated by Debye–Grüneisen models of Moruzzi et al. and of Wang et al. The entropies predicted from these two Debye models have a general agreement with about ±0.5 J/mol K differences for all the three structures.

1. Introduction

Mg–Al based alloys, possessing the best strength to weight ratio among the common structural materials, have received increasing attention due to their applications in automotive and aerospace industries. However, despite the high specific strength, these alloys have limited use as structural materials due to their poor creep resistance at high temperatures, mainly caused by the softening of the intermetallic phase $Al_{12}Mg_{17}$ at elevated temperatures [1,2]. Significant improvements can be achieved by alloying. Additions of rare earth elements show improvement in mechanical properties as a result of formation of strengthening precipitates [3,4], but they incur high costs. As a lower cost element, the addition of Ca provides additional ways to improve the creep resistance of Mg–Al base alloys through the replacement of the $Al_{12}Mg_{17}$ phase by more stable Laves phases [5,6]. Therefore, the ternary Mg–Al–Ca alloys have received increasing attention in the past few years, especially the Laves phases in Mg alloys due to their excellent physical and chemical properties [7]. Despite the interesting properties of these alloys, there are only quite a few existing theoretical investigations on the structures and stability of these Laves phases in the Mg–Al–Ca system and most of them were studied for 0 K [8,9].

To better understand the alloying behavior of Ca on Mg–Al alloys, it is important to determine the thermochemical properties of the Laves phases. A general two-sublattice model $(Mg, Al, Ca)_2(Mg, Al, Ca)_1$ is used to represent the Laves phases (C14, C15, and C36) with homogeneity ranges as discussed in [8,10]. It is found that the energetics for end-members with one element in each sublattice remain to be developed due to the lack of data, especially for the nonstable ones. In the current work, we present a systematic theoretical study on the structural, vibrational, and thermodynamic properties of A_2B type Laves phase with C14, C15, and C36 structures from first-principles. The total energies of all the nine end-members in the Laves phases C14, C15 and C36 structures are calculated and fitted by an equation of state (EOS). For the stable phases, e.g. C14-Mg_2Ca and C15-Al_2Ca, the vibrational properties are firstly predicted from phonon calculations. Subsequently, the Debye temperature evaluated from phonon properties is employed to adjust the scaling factor (s) in Debye–Grüneisen model by Moruzzi et al. [11]. Herein, the vibrational properties through Debye–Grüneisen model are compared with those obtained from phonon calculations. For nonstable end-members, it is impossible to perform either the phonon calculations or experiments to estimate their vibrational properties. However, from the analysis of thermodynamic properties for stable end-members, we propose to predict the thermodynamic properties of nonstable A_2B type Laves phases using Debye–Grüneisen model by Moruzzi et al. [11] and Wang et al. [12]. The results of this work are expected to enhance the understanding of phase stability in the Mg–Al–Ca ternary system, and the

* Corresponding author. Current address: Diamond Innovations, Worthington, OH, 43085, USA.
E-mail address: zhanghuipku@hotmail.com (H. Zhang).

0966-9795/$ – see front matter © 2011 Elsevier Ltd. All rights reserved.
doi:10.1016/j.intermet.2011.08.019

approaches developed are extensible to other materials and for developing self-consistent and robust thermodynamic databases.

The rest of the paper is organized as follows. In Section. 2, we present the theories to calculate the vibrational contribution using both phonon calculations and Debye models. The computational framework and simulation details are described in Section 3. In Section. 4, we discuss the EOS fittings and the calculated first-principles thermodynamic properties for these A_2B type Laves phases. Finally, we summarize the conclusions of the present work.

2. Methodology

Under the quasiharmonic approximation, the Helmholtz free energy, F, of a system at temperature T and volume V is given by [13–17]

$$F(V,T) = E_0(V) + F_{vib}(V,T) + F_{el}(V,T) \quad (1)$$

where $E_0(V)$ is the first-principles static energy at 0 K and volume V, $F_{vib}(V,T)$ the lattice vibrational contributions to the free energy, and $F_{el}(V,T)$ the thermal electronic contributions. Within the quasi-harmonic approximation, the anharmonic effect is accounted by the harmonic approximation at several volumes.

From phonon density of states, the lattice vibrational free energy can be calculated through [13–15]:

$$F_{vib}(V,T) = k_B T \int_0^\infty \ln\left[2\sinh\frac{\hbar\nu}{2k_B T}\right] g(\nu,V)\mathrm{d}\nu \quad (2)$$

where T is the temperature, k_B the Boltzmann constant, $\hbar$ the Planck constant, and $g(\nu,V)$ the phonon density of states as a function of phonon frequency ν and volume V.

The vibrational properties can be alternatively characterized by their Debye temperatures Θ_D [1,11,16]:

$$k_B\Theta_D(n) = h\nu_D(n) \quad (3)$$

$$\nu_D(n) = \left[\frac{n+3}{3}\int_0^\infty \nu^n g(\nu)\mathrm{d}\nu\right]^{1/n} \quad (n\neq 0, n> -3), \quad (4)$$

where $\nu_D(n)$ is the Debye cutoff frequency. The second moment cutoff frequency ($n = 2$) is used in this work, since$\Theta_D(2)$ corresponds to the Debye temperature obtained from heat capacity data [1,18].

Consequently, the vibrational Helmholtz free energy can be estimated by Debye model through the Debye temperature, Θ_D,

$$F_{vib}(V,T) = \frac{9}{8}k_B\Theta_D + k_B T\left\{3\ln\left[1-\exp\left(-\frac{\Theta_D}{T}\right)\right] - D\left(\frac{\Theta_D}{T}\right)\right\} \quad (5)$$

where $D(\Theta_D/T)$ is the Debye function with Θ_D determined by via phonon frequencies. In terms of Debye–Grüneisen model by Moruzzi et al. [11], Θ_D is given by:

$$\Theta_D = sAV_0^{1/6}\left(\frac{B_0}{M}\right)^{1/2}\left(\frac{V_0}{V}\right)^{\gamma} \quad (6)$$

where M is the atomic mass, s the scaling factor with a default value of 0.617 as discussed by Moruzzi et al. [11], γ the Grüneisen constant, V_0 the 0 K static equilibrium volume, B_0 the bulk modulus calculated at V_0, B'_0 the derivative of B_0 against P, $\gamma = ((1+B'_0)/2) - x$ with $x = 1$ for low temperatures and $x = 2/3$ for high temperatures [11].

Without using the Grüneisen constant, another method to calculate the Debye temperature was proposed by Wang et al. [12,16]:

Table 1
Details of the first-principles and phonon calculations, including the space group of pure elements and compounds [36], k-mesh used for the electronic and phonon structures, the number of atoms in the supercell (SC) for phonon calculations, the displacement (Δr) of disturbed atom from its equilibrium position, and the cutoff distance (R_{cut}) for the fitting range of force constants.

EOS Calc.	Space group	k-mesh electron	Phonon calc.	SC atoms	k-mesh phonon	Δr (Å)	R_{cut} phonon (Å)
Al	$Fm\bar{3}m$	35 × 35 × 35	Al	32	6 × 6 × 6	0.1	6
Ca	$Fm\bar{3}m$	22 × 22 × 22	Ca	32	6 × 6 × 6	0.1	7
Mg	$P6_3/mmc$	25 × 25 × 15	Mg	36	6 × 6 × 6	0.1	6
C14	$P6_3/mmc$	12 × 12 × 8	Mg_2Ca	48	5 × 5 × 5	0.1	7
C15	$Fm\bar{3}m$	12 × 12 × 12	Al_2Ca	48	4 × 4 × 4	0.1	7
C36	$P6_3/mmc$	11 × 11 × 4					

$$\Theta_D = sAV^{1/6}\left\{\frac{1}{M}\left[B - \frac{2(\lambda+1)}{3}P\right]\right\}^{1/2} \quad (7)$$

where B is the bulk modulus calculated from the 0 K static total energy curve at a given volume V, P the pressure calculated from the 0 K static total energy curve at V, $\lambda = -1, 0$, and 1 correspond to

Table 2
Calculated equilibrium volume (V_0), enthalpy of formation (ΔH), bulk modulus (B_0), and pressure derivative of bulk modulus (B_0') of binary laves phases at 0 K.

	Structure	V_0 (Å^3/atom)	ΔH (kJ/mol)	B_0 (GPa)	B'_0
Al	fcc	16.481		76.4	4.80
		16.322[a] [8]		78[b] [37]	4.2[b] [37]
		16.60[b] [36]			
Ca	fcc	42.163		17.4	3.27
		42.564[a] [1]		17[b] [38], 18.3[b] [39]	
Mg	hcp	23.043		34.4	4.02
		22.908[a] [1]		45[b] [38], 35.2[b] [39], 36.8[b] [40]	4.3[b] [40]
Al_2Ca	C14	21.583	−32.82	55.5	3.89
	C15	21.445	−34.42	56.2	4.22
		21.695[a] [8]	−33.98[a] [8][c]	56.65[a] [9]	6.78[a] [9]
		21.65[b] [36]			
	C36	21.451	−33.20	56.0	4.25
Mg_2Ca	C14	28.240	−12.02	30.3	4.06
		28.370[a] [1]	−12.06[a] [9],	30.54[a] [1],	4.01[a] [1],
		28.86[b] [36]	−12.3[a,c] [1]	31.06[a] [9], 31.4 [41]	4.07[a] [9]
	C15	28.325	−11.73	29.8	3.78
	C36	28.255	−11.97	30.2	3.92
Al_2Mg	C14	18.807	−1.98	60.3	4.40
	C15	18.827	−1.56	61.1	4.47
	C36	18.822	−2.12	61.0	4.44
Mg_2Al	C14	21.732	26.10	37.4	4.24
	C15	21.693	25.32	38.2	4.19
	C36	21.697	25.51	38.0	4.27
Ca_2Mg	C14	37.532	29.82	14.7	3.46
	C15	38.345	30.82	14.3	3.34
	C36	37.946	30.30	14.6	3.43
Ca_2Al	C14	32.352	36.36	11.2	6.71
	C15	33.220	46.93	15.9	3.39
	C36	32.405	45.34	11.1	4.25
Al_2Al	C14	17.498	14.09	67.9	4.18
	C15	17.472	15.57	64.6	4.61
	C36	17.463	14.95	65.1	4.85
Mg_2Mg	C14	23.739	7.49	34.0	4.00
	C15	23.722	7.21	34.2	4.10
	C36	23.718	7.30	34.0	4.21
Ca_2Ca	C14	39.460	8.45	18.2	3.39
	C15	44.172	8.49	16.0	3.18
	C36	44.017	8.32	16.1	3.34

[a] Calculated results at 0 K from references.
[b] Experimental results at 298 K.
[c] Experimental results at 298 K are in Table 4.

the thermodynamic theories of Slater [19], Dugdale and MacDonald [20], and the free volume theory [21], respectively. It should be noted that the case of $\lambda = -1$ by Wang et al. [12] is equivalent to the high temperature case by Moruzzi et al. [11] and that the case of $\lambda = 0$ by Wang et al. [12] is equivalent to low temperature case by Moruzzi et al. [11]. Since the present interest is focused at the relatively high temperature region of the phase diagram, all the calculations using Debye–Grüneisen models of Moruzzi et al. [11] and of Wang et al. [12] are carried out at high temperature with $x = 2/3$ and $\lambda = -1$, respectively. When possible, the scaling factors for the Debye–Grüneisen models are determined by making the Debye temperatures from Equation (6) or Equation (7) equal to the Debye temperature obtained by phonons (Equation (4)).

3. First-principles computational details

In the present work, first-principles calculations were performed by using the projector-augmented wave (PAW) method as implemented in VASP [22,23]. The generalized gradient approximation (GGA) of Perdew-Burke-Ernzerhof (PBE) [24] is used for the exchange-correlation functional. The electronic configurations considered are $3s^2 3p^1$ for Al, $3s^2$ for Mg, and $3p^6 4s^2$ for Ca, respectively. We use the energy cutoff of 320 eV, i.e., 1.3 times the highest energy cutoff among Al, Mg and Ca as suggested by VASP. The crystal structures of Laves C14, C15, and C36 are summarized in Table 1. The Monkhorst-Pack scheme is used for the Brillouin-zone integrations [25] of Al, Ca, Laves C15 and Laves C36, while Γ centered k-mesh is used for Mg and Laves C14.

The phonon calculations of C14-Mg_2Ca and C15-Al_2Ca are carried out by using the supercell method implemented in the ATAT package [26] with VASP code as the computational engine. The supercell method is based on the frozen phonon approximation through which the changes in forces acting on atoms are calculated in the direct space by displacing the atoms from their equilibrium positions. Table 1 shows the detailed settings for first-principles calculations, including the space group, the size of k-mesh for electronic structure calculations and in the perturbed supercell for

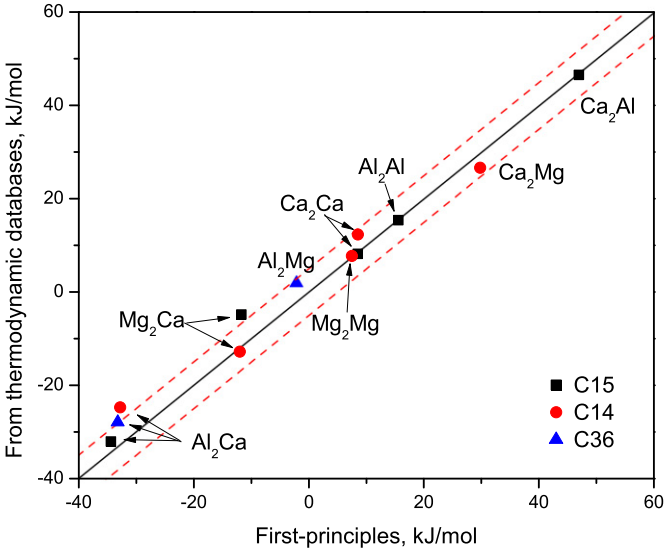

Fig 1. Enthalpies of formation for the Al–Mg–Ca ternary system in a variety of Laves structures. Where C15 structures of Al_2Ca, Al_2Al, Ca_2Al, and Ca_2Ca are from the thermodynamic database by Ozturk et al. [30], while C14 structures of Mg_2Ca, Mg_2Mg, Ca_2Mg and Ca_2Ca are from the thermodynamic database by Zhong et al. [31], and C14-Al_2Ca, C15-Mg_2Ca, C36 structures of Al_2Mg, and Al_2Ca are from the thermodynamic database by Janz et al. [29].

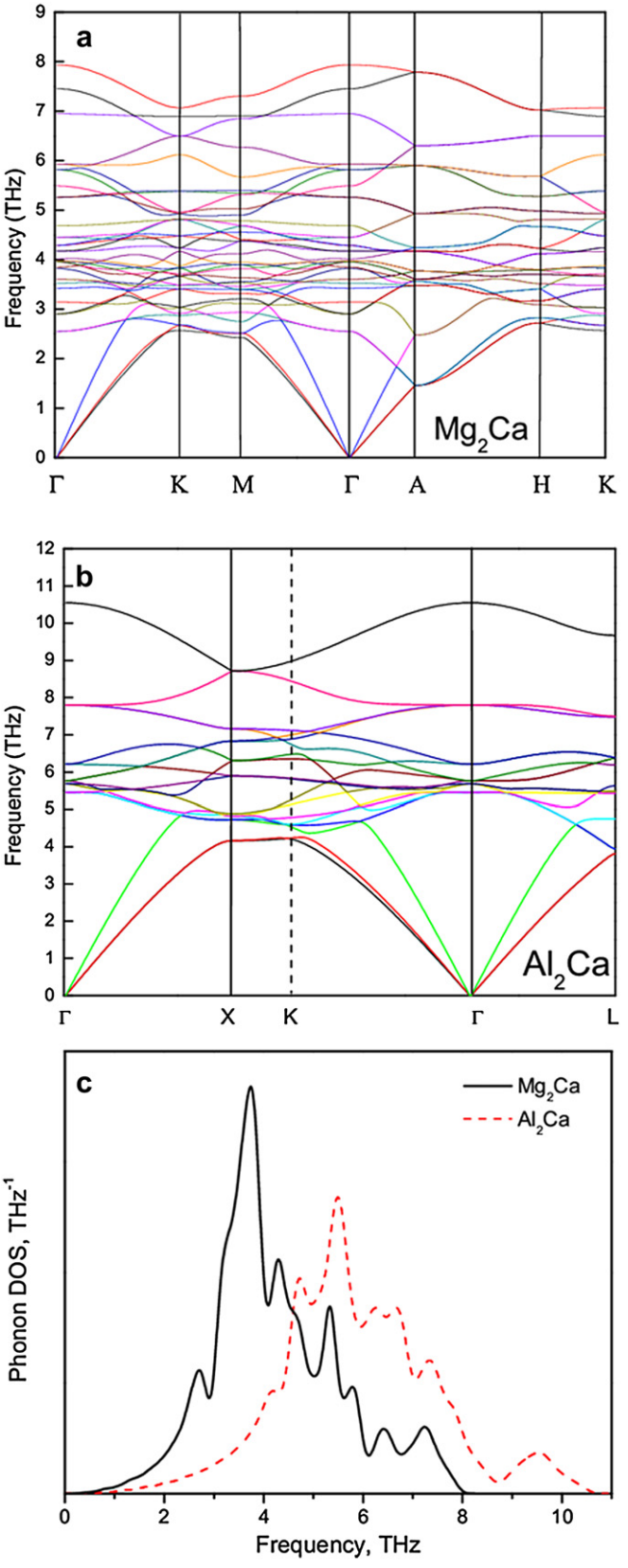

Fig. 2. (a) Calculated phonon dispersion curves of C14-Mg_2Ca. (b) Calculated phonon dispersion curves of C15-Al_2Ca. (c) Phonon DOS's of the C14-Mg_2Ca and C15-Al_2Ca at their equilibrium volumes at 298 K.

Table 3
Debye frequency and Debye temperatures of Al, Mg, Ca, C14-Mg_2Ca, and C15-Al_2Ca.

	Debye temperature (K)		Debye cutoff frequency (THz)	
	Calc.[a]	Exp.	Calc.	Exp.
Al	400	396 [42]	8.33	8.35 [42]
Mg	323	325 [42], 323 [18], 320 [1]	6.73	6.67[b]
Ca	210	210 [43], 229 [44]	4.40	4.48 [1]
C14-Mg_2Ca	277		5.78	
C15-Al_2Ca	377		7.86	

[a] Derived from the second moment of phonon DOS.
[b] Calculated Debye cutoff frequency from the eighth neighbor Born–von Karman model.

phonon calculations, the number of atoms in the supercell for phonon calculations; the setting of displacement from the equilibrium atomic position, and the cutoff distance used to fit the force constants and phonon properties.

4. Results and discussion

4.1. Evaluation of enthalpies for all end-members

The total energy of each end-member is calculated as a function of volume and fitted by the 4-parameter Birch–Murnaghan equation of state [16,27,28]:

$$E(V) = a + bV^{-2/3} + cV^{-4/3} + dV^{-6/3} \quad (8)$$

In the present work, 6 data points in the volume range of 0.88–1.19 V_0 are used for the EOS fitting for each structure. The structural properties including the equilibrium volume, enthalpy of formation, bulk modulus and its pressure derivative for each end-member at 0 K are determined, and compared with available data as listed in Table 2. Note that most of B'_0 values are 3–6, which is within the range of values for nearly all the materials. Additionally, the EOS fitting error is estimated by $\sqrt{\sum_i [(C_i - B_i)/B_i]^2/N}$, where C_i and B_i are the fitted value and first-principles predicted value, respectively. N represents the total number of data points. It is worth mentioning that the EOS fitting errors are smaller than 1×10^{-4}, in all cases. Fig. 1shows the calculated enthalpy of formation of each A_2B type Laves phase, in comparison with the CALPHAD modeled results for the Mg–Al–Ca [29], Al–Ca [30], and Mg–Ca [31] databases. The solid line represents the perfect agreement between the first-principles values and CALPHAD assessments, and two dashed lines define an error bar of ±5 kJ/mol. The value of ±5 kJ/mol is chosen due to the uncertainty for most experimental studies of enthalpies of formation. The calculated results compared favorably with each other with the differences within ±5 kJ/mol except for the C14-Al_2Ca and C15-Mg_2Ca phases. Such discrepancy is due to the arbitrary enthalpies of formation values used in CALPHAD assessments since both of these two are nonstable phases. The enthalpies of formation of C14, C15, and C36 structures with the same composition have similar values with those for Al_2Ca, Mg_2Ca, and Al_2Mg being negative. Al_2Ca has the lowest enthalpy of formation in their respective structures with the value being the lowest for the C15 structure, which is consistent with its stability in the Al–Ca binary system [30]. For the composition of Mg_2Ca, the C14 structure has the lowest energy among three structures, which is consistent with the fact that it is the stable phase in the Mg–Ca system [31]. As for V_0 and B_0, all the calculations reveal the same trend: the one with the larger equilibrium volume showing lower bulk modulus.

4.2. Evaluation of entropies for all end-members at 298 K

Fig. 2(a) and (b) show the phonon dispersion curves of C14-Mg_2Ca and C15-Al_2Ca at their equilibrium volumes at 298 K, 28.86 Å^3/atom [36] and 21.65 Å^3/atom [36], respectively. Al_2Ca has the higher frequency due to the influence of mass. The phonon density of states (DOS's) for C14-Mg_2Ca and C15-Al_2Ca are shown in Fig. 2(c). We note that in the low frequency region, the phonon DOS of C14-Mg_2Ca has higher values than that of C15-Al_2Ca, indicating that C14-Mg_2Ca has the larger phonon contributions to Gibbs energy from the vibrational entropy [32]. In principle, the higher value of the phonon density of states in the lower frequency region implies a weak bonding nature and correspondingly a lower Debye temperature [15]. Table 3 summarizes the estimated second

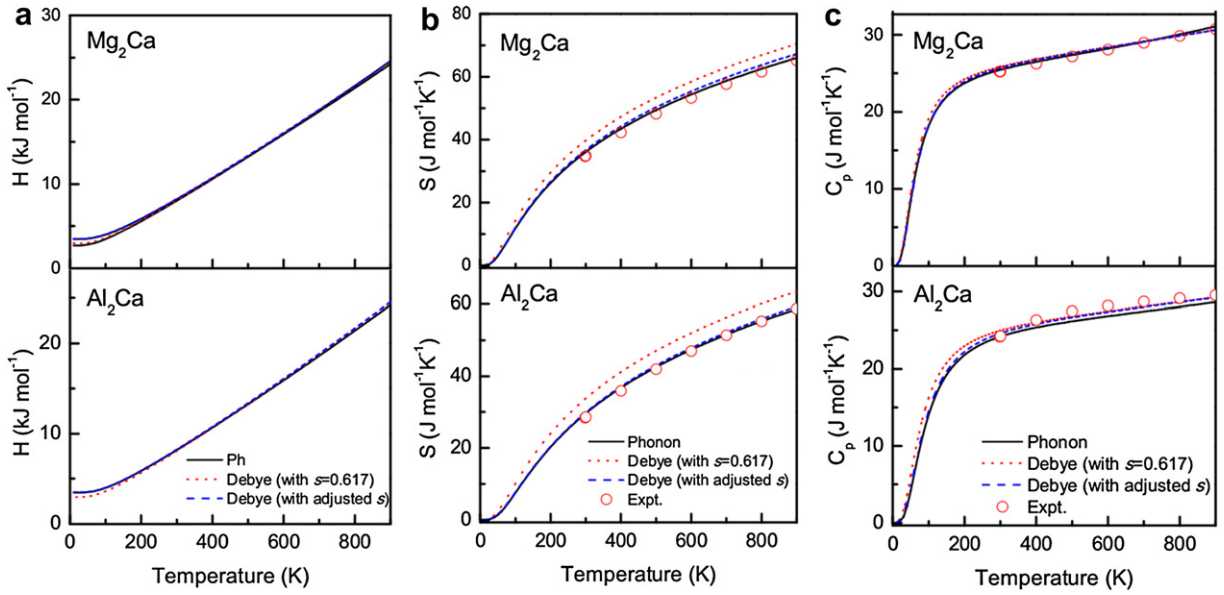

Fig. 3. Thermodynamic properties of vibrational enthalpy (H), entropy (S), and heat capacity (C_p) for Al_2Ca and Mg_2Ca from phonon calculations (—), Debye model with $s = 0.617$ (….), and Debye model with adjusted s (- - -) together with available experiments (○) [33].

Table 4
Thermodynamic properties of stable intermetallic compounds at 298 K.

		V_{298} (Å^3/atom)	ΔH (kJ/mol)	ΔS (J/mol)	B^T (GPa)	C_P (J mol^{-1}K^{-1})	α_L (10^{-6}K^{-1})
C14-Mg_2Ca	Phonon	28.953	−12.12	−0.68	27.0	24.95	27.32
	Debye_Grü ($\gamma = 0.67$)	29.043	−12.17	−0.84	28.0	25.10	29.45
	Debye_Grü ($\gamma = 0.617$)	29.037	−12.10	−0.54	28.0	25.24	29.73
	Ref.	31.134	−13.5 ± 0.42 [45], −12.7 ± 0.63 [46], −13.0 ± 0.88 [47] −12.44 [1]	−0.99 [33], −1.7 [31] −0.46 [1]	27.71 [1]	25.20 [1], 24.58	25.72 [1]
C15-Al_2Ca	Phonon	21.840	−34.70	−3.99	51.9	11.91	18.22
	Debye_Grü ($\gamma = 0.7$)	21.917	−34.60	−3.52	52.8	12.11	21.65
	Debye_Grü ($\gamma = 0.617$)	21.911	−34.56	−2.71	52.8	12.29	21.97
	Ref.	21.655	−31.3 ± 0.5 [48], −33.4 ± 0.6 [49], −34.3 ± 3.5 [50], −29.4 ± 0.9 [51]	−5.02 [30]			

moment Debye temperatures at the theoretical equilibrium volumes from phonon calculations. It is shown that C14-Mg_2Ca has a lower Debye temperature, confirming again its weaker bonding than that of C15-Al_2Ca.

By using the calculated Debye temperatures from phonon, the scaling factor, s, in Debye–Grüneisen model can be adjusted, with the value of 0.67 and 0.7 for C14-Mg_2Ca and C15-Al_2Ca, respectively. The temperature dependent vibrational enthalpies, entropies, and heat capacities of C15-Al_2Ca and C14-Mg_2Ca are shown in Fig. 3, including the ones from phonon calculations, Debye–Grüneisen model with the suggested scaling factor ($s = 0.617$) by Moruzzi et al. [11], and Debye–Grüneisen model with the adjusted s. Note that the thermal electronic contributions are included in this work. The calculated vibrational enthalpies shown in Fig. 3(a) are almost identical regardless of calculation methods. In Fig. 3(b), the entropy is calculated from $S = -(\partial F/\partial T)_V$ under $P = 0$. The predictions from phonon calculations and Debye–Grüneisen model using the adjusted s show consistency and are in good agreement with recommended values (0.617) [33] as well. Regarding the Debye–-Grüneisen model using the suggested s ($s = 0.617$), the evaluated entropies are slightly higher than those from phonon calculations, e.g. about 6.2% and 7.7% for Mg_2Ca and Al_2Ca at 900 K, respectively. The heat capacity at constant pressure is estimated by $C_P = C_V + \beta^2 BTV$, where C_V is the heat capacity at constant volume calculated by $C_V = -T(\partial S/\partial T)_V$, and β, B, T, and V are the volume thermal expansion coefficient, bulk modulus, temperature and volume, respectively.

Table 4 summarizes the calculated equilibrium volume, enthalpy of formation, entropy of formation, bulk modulus, heat capacity, and linear thermal expansion at 298 K for both C15-Al_2Ca and C14-Mg_2Ca. Vibrational contributions evaluated from phonon calculations, Debye–Grüneisen model with the adjusted s, and Debye–Grüneisen model with the suggested $s = 0.617$ [11] are also compared in Table 4, showing the consistent prediction of thermodynamic properties and good agreement with the available experimental data as well. At room temperature, the larger volume, the lower bulk modulus, and the lower enthalpy of formation of C14-Mg_2Ca with respect to those of C15-Al_2Ca confirm again the weaker bonds in C14-Mg_2Ca. By considering the thermodynamic properties of stable C15-Al_2Ca and C14-Mg_2Ca, it is found that (i) with the phonon and thermal electronic contributions included, the thermodynamic properties can be well described; (ii) the vibrational enthalpy and heat capacity calculated from the suggested scaling factor (s) are almost identical with the ones

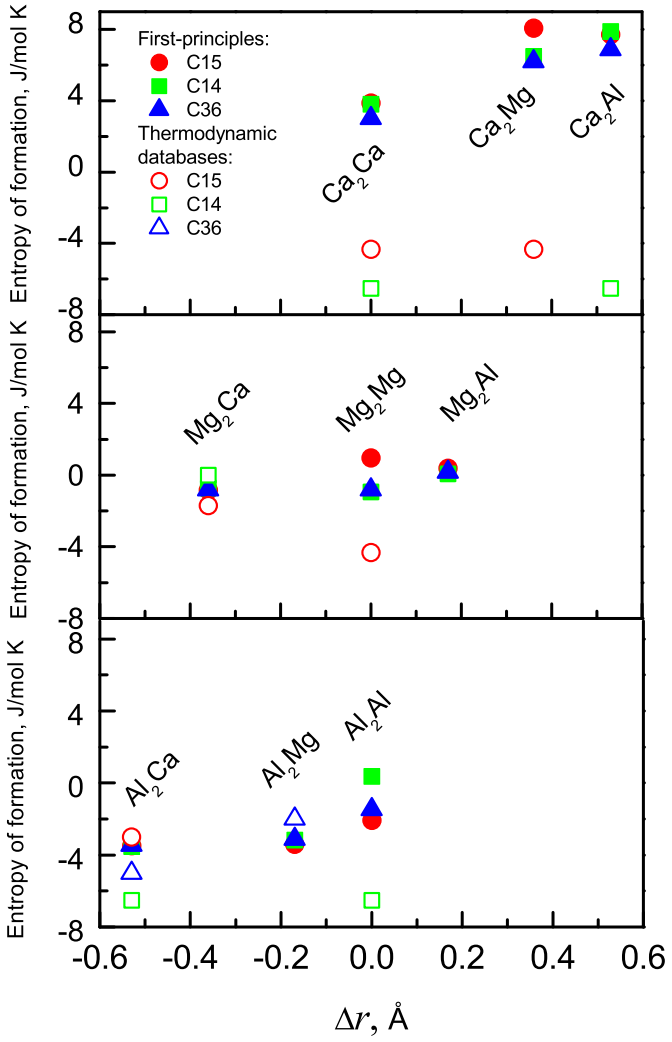

Fig. 4. Entropies of formation at 298 K for the end-members in the Al–Mg–Ca ternary system plotted with respect to their relative pure elements, in comparison with the values from thermodynamic databases. Where C15 structures of Al_2Ca, Al_2Al, Ca_2Al, and Ca_2Ca are from the thermodynamic database by Ozturk et al. [30], while C14 structures of Mg_2Ca, Mg_2Mg, Ca_2Mg and Ca_2Ca are from the thermodynamic database by Zhong et al. [31], and C14-Al_2Ca, C15-Mg_2Ca, C36 structures of Al_2Mg, and Al_2Ca are from the thermodynamic database by Janz et al. [29].

calculated with adjusted s in Debye–Grüneisen model and in good agreement with phonon calculations and experiments, and (iii) the entropy predicted by Debye–Grüneisen model with $s = 0.617$ is about 6∼7% higher than that from Debye–Grüneisen model with adjusted s at high temperature (900 K).

Except C14-Mg_2Ca and C15-Al_2Ca phases, the other end-members with A_2B type Laves structures are not stable in the Mg–Al–Ca system, and hence their vibrational properties cannot be obtained from phonon calculations. In the present work, their thermodynamic properties are investigated by the Debye–-Grüneisen model with the scaling parameter $s = 0.617$ [11]. The calculated entropies of formation for each A_2B structure at 298 K are shown in Fig. 4 as a function of difference in metallic radius between A and B, Δr, in comparison with those calculated from the Al–Ca [30], Mg–Ca [31], and Al–Mg–Ca [29] databases. The discrepancies are expected especially for the nonstable phases as there were no experimental data to evaluate the entropies of formation of non-stable structures in the database development. For example, entropies of formations of nonstable C15-Al_2Al, C15-Ca_2Ca, and C15-Ca_2Al are assumed to be the same as the stable phase C15-Al_2Ca. It is observed that Al_2B has the most negative values of entropies of formation, while Ca_2B has the most positive values. In each group of Al_2B, Mg_2B, and Ca_2B, we note that the entropy of formation becomes less negative (more positive) when Δr increases. It can be understood that when the atom B is smaller than the atom A in A_2B, the contact between the B atom and its neighbors becomes poorer resulting in weak A–B bonding and high entropy. The relationship between entropy of formation and Δr in $L1_2$ phases also shows a similar trend [34].

The bonding strength can be alternatively illustrated by bulk modulus since bulk modulus is proportional to the average stretching force constant [35]. In Fig. 5, bulk modulus of a compound with respect to its pure elements, e.g. $\Delta B(Al_2Ca) = B(Al_2Ca) - {}^2/_3\,B(Al) - {}^1/_3\,B(Ca)$, are presented as a function of Δr. It is shown that ΔB becomes more negative as Δr increases, showing weaker bonding in the compound. From both Figs 4and 5, the relationship between ΔS and ΔB are illustrated in Fig. 6, demonstrating that the stronger bonding of a compound can be represented by a more positive (less negative) ΔB with a more negative (less positive) ΔS.

For phases with the same element A in A_2B, it is worth noting that the more negative entropy of formation corresponds to a more negative enthalpy of formation (see Table 2). A more negative enthalpy of formation is an indicator of a stronger interatomic bonding and stronger bonding leads to lower vibrational entropies, and hence a more negative entropy of formation.

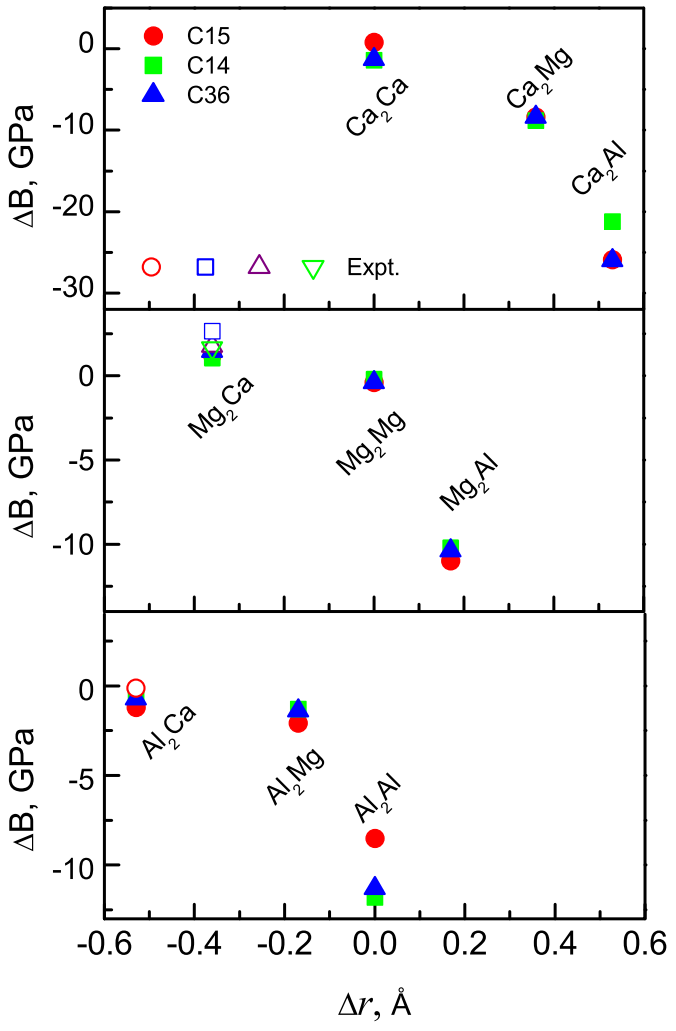

Fig. 5. Bulk modulus relatively to its pure elements for the end-members in the Al–Mg–Ca ternary system in comparison with the available data (△ [1] ▽ ○ [9] and □ [41]) in the literature.

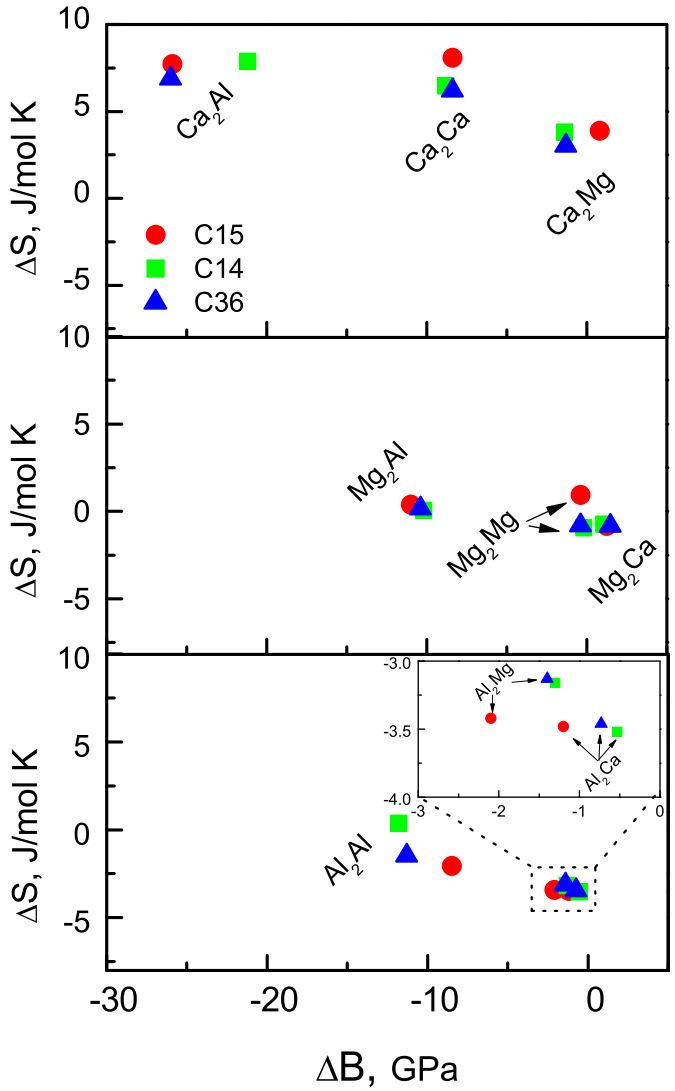

Fig. 6. Entropies of formation at 298 K for the end-members in the Al–Mg–Ca ternary system as a function of bulk modulus relative to its pure elements.

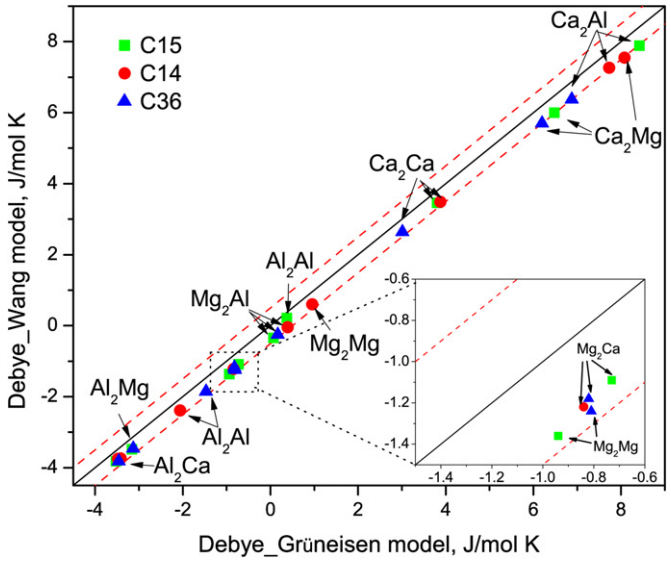

Fig. 7. Comparison of calculated entropies of formation at 298 K for the end-members in the Mg–Al–Ca systems from Debye–Grüneisen models by Moruzzi et al. [11] and by Wang et al. [12]. The solid line shows unity ($y = x$) while the dashed lines present an error range of ±0.5 J/mol K.

Furthermore, the entropies of formation of A_2B are also estimated by the Debye–Grüneisen model of Wang et al. and compared with Debye–Grüneisen model of Moruzzi et al. in Fig. 7. A perfect agreement between the calculated and experimental values is indicated by the solid line, where an error bar of ±0.5 J/mol K are shown by the dashed lines. The calculated entropies of formation from two models are consistent with each other, and the differences are within ±0.5 J/mol K in all cases.

5. Summary

In the present work, a systematic analysis on the structural, vibrational, and thermodynamic properties of the A_2B type Laves phases with C14, C15, and C36 structures in the Mg–Al–Ca system has been performed using first-principles methods. Energy vs. volume (E–V) equations of state (EOS) are fitted to the first-principles calculations. Through the use of the supercell method with quasiharmonic corrections, the vibrational properties of fcc-Al, hcp-Mg, fcc-Ca, C14-Mg_2Ca, C15-Al_2Ca are calculated. It is shown that C14-Mg_2Ca has weaker bonds with respect to C15-Al_2Ca, which is confirmed by its larger volume, lower bulk modulus, and lower enthalpy of formation. Furthermore, a comparative study of stable structures is performed between phonon and Debye–Grüneisen model with scaling parameter adjusted from phonon calculation and suggested in the literature. It is found that those calculations show the consistent thermodynamic properties of C14-Mg_2Ca and C15-Al_2Ca. In addition, the thermodynamic properties of the nonstable A_2B type Laves structures are predicted by both Debye_Grüneisen and Debye–Wang models.

Acknowledgments

This work was funded by the National Science Foundation (NSF) through Grants Nos. DMR-0510180. First-principles calculations were carried out partially on the LION clusters supported by the Materials Simulation Center and the Research Computing and Cyber infrastructure unit at Pennsylvania State University, and partially on the resources of NERSC supported by the Office of Science of the U. S. DOE under contract No. DE-AC02-05CH11231.

References

[1] Arroyave R, Liu ZK. Phys Rev B 2006;74:174118.
[2] Zhang H, Shang SL, Wang Y, Saengdeejing A, Chen LQ, Liu ZK. Acta Mater 2010;58:4012.
[3] Luo AA. Int Mater Rev 2004;49:13.
[4] Mordike BL, Ebert T. Mater Sci Eng A 2001;302:37.
[5] Ozturk K, Zhong Y, Luo AA, Liu ZK. JOM 2003;55(11):A40.
[6] Zhong Y, Luo AA, Sofo JO, Liu ZK. Magnesium - Sci Technol Appl 2005; 488-489:169.
[7] Amerioun S, Simak SI, Haussermann U. Inorg Chem 2003;42:1467.
[8] Zhong Y, Liu J, Witt RA, Sohn YH, Liu ZK. Scripta Mater 2006;55:573.
[9] Yu WY, Wang N, Xiao XB, Tang BY, Peng LM, Ding WJ. Solid State Sci 2009;11: 1400.
[10] Ansara I, Chart TG, Guillermet AF, Hayes FH, Kattner UR, Pettifor DG, et al. CALPHAD 1997;21:171.
[11] Moruzzi VL, Janak JF, Schwarz K. Phys Rev B 1988;37:790.
[12] Wang Y, Ahuja R, Johansson B. Int J Quantum Chem 2004;96:501.
[13] Wang Y, Liu ZK, Chen LQ. Acta Mater 2004;52:2665.
[14] Baroni S, de Gironcoli S, Dal Corso A, Giannozzi P. Rev Mod Phys 2001;73: 515.
[15] Shang S, Wang Y, Arroyave R, Liu ZK. Phys Rev B 2007;75:092101.
[16] Shang SL, Wang Y, Kim D, Liu ZK. Comput Mater Sci 2010;47:1040.
[17] Wang Y, Wang JJ, Zhang H, Manga VR, Shang SL, Chen LQ, et al. J Phys Condens Matter 2010;20:225404.
[18] Dederichs PH, Schober H, Sellmyer DJ. In: Hellwege KH, Olsen JL, editors. Metals: phonon states, electron states and fermi surfaces. Berlin: Springer-Verlag; 1981.
[19] Slater JC. Introduction to chemical physics. New York: McGraw-Hill; 1939.
[20] Dugdale JS, Macdonald DKC. Phys Rev 1953;89:832.
[21] Vashchenko VY, Zubarev VN. Sov Phys Solid State 1963;5:653.
[22] Kresse G, Furthmuller J. Comput Mater Sci 1996;6:15.
[23] Kresse G, Furthmuller J. Phys Rev B 1996;54:11169.
[24] Perdew JP, Wang Y. Phys Rev B 1992;45:13244.
[25] Monkhorst HJ, Pack JD. Phys Rev B 1976;13:5188.
[26] van de Walle A, Asta M, Ceder G. CALPHAD 2002;26:539.
[27] Teter DM, Gibbs GV, Boisen MB, Allan DC, Teter MP. Phys Rev B 1995;52: 8064.
[28] Mei ZG, Shang SL, Wang Y, Liu ZK. Phys Rev B 2009;79.
[29] Janz A, Grobner J, Cao H, Zhu J, Chang YA, Schmid-Fetzer R. Acta Mater 2009; 57:682.
[30] Ozturk K, Zhong Y, Chen LQ, Wolverton C, Sofo JO, Liu ZK. Metall Mater Trans A 2005;36A:5.
[31] Zhong Y, Ozturk K, Sofo JO, Liu ZK. J Alloy Compd 2006;420:98.
[32] Shang SL, Wang Y, Du Y, Liu ZK. Intermetallics 2010;18:961.
[33] Barin I. Thermochemical data of pure substances. Weinheim, New York: 1995.
[34] Bogdanoff PD, Fultz B. Philos Mag B-Phys Condens Matter Stat Mech Electron Opt Magn Prop 1999;79:753.
[35] El-Moneim A Abd. Mater Chem Phys 2001;70:340.
[36] Villars PP. Pearson's handbook of crystallographic data for intermetallic phases. American Society for Metals; 1985.
[37] Gerward L. J Phys Chem Solids 1985;46:925.
[38] Winter MJ. WebElements, in, www.webelements.com.
[39] Chen Q, Sundman B. Acta Mater 2001;49:947.
[40] Errandonea D, Meng Y, Hausermann D, Uchida T. J Phys Condes Matter 2003; 15:1277.
[41] Sumer A, Smith JF. J Appl Phys 1962;33:2283.
[42] Seitz F, Turnbull D. Solid. State. Physics. New York: Academic Press; 1964.
[43] Cook JG, Vanderme. Mp. J Phys F Met Phys 1973;3:130.
[44] White GK. J Phys F Met Phys 1972;2:865.
[45] King RC, Kleppa OJ. Acta Metall 1964;12:87.
[46] Gartner GJ. Thesis, in, Iowa State University, 1965.
[47] Davison JE, Smith JF. Trans Metall Soc AIME 1968;242:2045.
[48] Veleckis E. J Less Common Met 1981;80:241.
[49] Notin M, Mejbar J, Bouhajib A, Charles J, Hertz J. J Alloy Compd 1995;220:62.
[50] Notin M, Hertz J. CALPHAD 1982;6:49.
[51] Kevorkov D, Schmid-Fetzer R, Pisch A, Hodaj F, Colinet C. Z Metallkd 2001;92: 953.